

EFFECT OF PISTON DEEP-BOWL ECCENTRICITY ON THE IN-CYLINDER  
AIR MOTION DURING COMPRESSION STROKE OF  
RECIPROCATING DIESEL ENGINE

تأثير انحراف غرفة الاحتراق على حركة الهواء داخل ماكينات الديزل خلال

تسرب الانضغاط

By

M. S. El Kady

Mechanical Engineering Department, Faculty of Engineering  
Mansoura University

خلاصة - بعد مريان الماشع داخل اسطوانة آلة الاحتراق الداخلي أهم العوامل التي تتحكم في عملية الاحتراق ولذا فإن لها التأثير الأكبر في تشغيل وعمل الآلة ، هذا السحب عرضي رأسير الفير مركزية لغرفة احتراق عمارة من فتحة عميقة اسطوانة في المكس على مريان الماشع داخل اسطوانة ذات حعن مفاثر للوجود وذلك أثناء تسرب الانضغاط . تتم تجسير انحراف مركز غرفة الاحتراق من مركز الاسطوانة من صغر الي ٣٠ مم بنسبة سطل الي ١٠٠ بمقد قطر المكس وذلك لعنجه نسبة نصف قطرها الي نصف قطر المكس تعادل ١٠٠. تتم الانضغاط تعسير رأسي بصغ سرعة الحقن للماشع في حالة غرف الاحتراق العسر مركزية وكذلك تم عرض تأثير نسبة انحراف مركز غرفة الاحتراق على التوزيع الزمني والغراسي لسرعة السران وسرعة الحقن للماشع والسرعة العماسية وكذلك خطوط منجعات البرعسة ومركز الدوامات وعندها في مختلف قطاعات غرفة الاحتراق العميقة .

#### ABSTRACT

The flow field within the cylinder of internal combustion engines is the most important factor controlling the combustion process. Thus it has a major impact on engine operation. This paper represents the influence of the piston deep bowl eccentricity on the in-cylinder flow in a deep-bowl direct injection chamber during the compression stroke. The eccentricity of the bowl axis is varied from 0 to 30 mm with a ratio to the piston radius of 0.5 with a diametral ratio of bowl to piston of 0.4. An expression for the squish flow velocity is obtained for the eccentric deep bowl. The influence of the eccentricity on the spatial and temporal distribution of the flow, the squish flow velocity, the tangential swirl velocity of the flow, the velocity vector and contour lines, the swirl center and the swirl intensity is represented .

#### 1. INTRODUCTION

Understanding in-cylinder fluid mechanics is a necessary step in predicting the performance of the spark ignition and Diesel engines. The flow field within the cylinder is the most important factor controlling the combustion process. It governs

the flame propagation rate in homogeneous charge spark-ignition engines; it controls the fuel-air mixing and burning rates in diesels. It influences the mechanisms by which many of the important emissions form. This flow pattern also governs the rate of heat transfer to the cylinder wall. Creation of the specific highly turbulent, flow field required for combustion affects the breathing capacity of the engine and hence its maximum power. These flows are extremely complex: they are turbulent, unsteady, and three dimensional, whereas the flow field itself largely depends on the geometrical shape of the cylinder. A high-speed direct injection diesel engine makes full use of air motion such as induction swirl and squish motion induced during the compression stroke to assist mixture formation and combustion. For this purpose a deep-bowl chamber as indicated in figure 1 is often employed. A relatively small and deep cavity in the piston can create a squish motion during the compression stroke when the piston approaches the cylinder head bringing about a toroidal vortex in the bowl cavity. A reversible squish may also be formed during the expansion stroke when the gas outflows from the cavity, and affects the fuel distribution to a certain extent [1]. In the case when an induction swirl is produced, the piston motion reinforces the swirl when the air is conveyed into the cavity, because of a decrease in the radius of rotation under the condition of a fixed angular momentum.

Recently more and more trials are being made to investigate the flow in the in-cylinder through numerical simulation but many of them still assume two dimensional or axisymmetrical flows [1,8]. The three dimensional flow in the eccentric deep bowl cavity is simulated also numerically in [9,10]. These computations reasonably reproduce the in-cylinder flow and reveal the details of the swirl and squish motions in the piston bowl. To have better insight into this in-cylinder flow further computations have been carried out and the numerical simulation system which is developed in [10] is used in this paper to assess the influence of the deep bowl eccentricity on the in-cylinder turbulent air motion during compression.

## 2. ENGINE CONDITIONS

For simplicity, the piston bowl is assumed to have a rectangular cross section as shown in fig. 1. A forced vortex flow around the cylinder axis with a uniform turbulence is assumed to represent the induction swirl when the inlet valve closes. It is also assumed that the working fluid is ideal air and no combustion takes place.

All computations were performed with a small size direct injection diesel engine having a small cylinder diameter = 120 mm, a stroke = 120mm and a length ratio of connecting rod to crank arm = 3.3. The base line conditions are as follows, the compression ratio = 16, the piston head clearance at TDC = 7.2 mm, diametral ratio of bowl to piston = 0.4 and engine speed = 2400 rpm. The eccentricity of the bowl axis to the cylinder axis is varied and took the values 0.0, 10.5, 15, 20 and 30 mm with a

ratio to the piston radius of 0, 0.175, 0.25, 0.333 and 0.5 respectively and the computation is done for a swirl ratio  $\omega_0$  of 0.6.

### 3. RESULTS OF COMPUTATIONS

#### 3.1 The squish flow

Near the top dead center, the charge between piston crown and cylinder head is squeezed radially inwards as a jet flow, which is usually called a squish flow and utilized to improve the combustion process due to the accompany violent turbulence. The theoretical squish velocity was calculated by Fitzgeorge [11] for the axisymmetrical bowl in piston chamber. For the eccentric bowl in piston chamber the squish flow velocity can be calculated under the following assumptions:

1. Dividing the cylinder volume into two volumes, the volume of the space between the piston ring and the cylinder head which is called squish volume  $V_s$  and the cavity plus the volume over the cavity to the cylinder head which is called the combustion volume  $V_c$ .

2. Equalizing the mass flow rate of the air flowing through the area between the two volumes to the decrease in the mass of the air of the squish volume.

3. Presuming a quasi-steady flow across an element of the vertical plane between the  $V_s$  and  $V_c$  the squish velocity  $U_s$  can be then obtained by the following relations

$$U_s/U_m = \frac{R_e^2 - r^2}{R^2 - r^2} \quad (1)$$

$$\text{with } R_e = \sqrt{R^2 - e^2 \sin^2 \theta} - e \cos \theta \quad (2)$$

$$\text{and } U_m/S_p = \frac{A_p}{A_m} \frac{E}{E + h/h_m} \quad (3)$$

Figure 2 shows the behavior of the mean squish flow velocity during the compression stroke. The mean squish flow velocity  $U_m$  increases firstly very slowly during the compression phase until 30°CA BTDC where it begins to increase rapidly and reaches its maximum value approximately at 10° BTDC. For the considered example this maximum value equals about 7 times the value of the mean piston speed. After this value it decreases sharply and vanishes at the TDC.

For the eccentric cavity the value of the radius  $R_e$  changes with the change of the angle  $\theta$  as shown in figure 1 and equation (2). This causes the change of the squish flow velocity along the plane dividing the squeezing volume and the combustion volume.

Figure 3 shows the behavior of the squish flow velocity  $U_s/U_m$  with the change of the angle  $\theta$  from 0 to 180° for the different eccentricity values. By  $\theta=0$   $R_m$  takes its maximum value and the maximum squish velocity occurs, then by the increase of the angle  $\theta$   $R_m$  decrease and also the squish flow velocity  $U_s$  decreases until it takes its minimum value at  $\theta=180^\circ$ .

Figure 4 shows the maximum and minimum values of the squish flow velocity by the different values of eccentricity. The maximum value of the squish flow velocity increases with the increase of the eccentricity and reaches by  $e=15\text{mm}$  the value 1.6 times its value at the axisymmetric case and by  $e=36\text{mm}$  the value 2.28.

### 3.2 The tangential velocity $V$

Figure 5 show the computed tangential velocity in the symmetrical section A-A for three crank angles 20°, 10° before TDC and the TDC for the eccentricity ratios of 0, 0.175, 0.25 and 0.33 also at three sections in the bowl cavity, the top of the cavity with  $k=5$ , and nearly one third and two thirds of its height where  $k=9$  and  $k=13$ . Roughly speaking there is a common inclination that may be observed from the figure that the velocity profiles are close to that of a rigid-body rotation in the central region while they deviate to a flat distribution on the outer region. The eccentricity of the deep bowl cavity decreases the tangential velocity at the right side and increases it at the left side. Figure 5 shows also that the change in the tangential velocity due to the increase of the eccentricity becomes always smaller with the proceeding of the flow towards the bottom of the cavity.

Figure 5 shows also that with the proceeding of the crank angle during the compression the change of the tangential velocity due to the increase of the eccentricity from 10.5 to 20 mm increases at the top of the cavity until 20° before TDC and then decreases again towards the TDC. While this change in the tangential velocity is somewhat smaller at  $k=9$  and is very small at  $k=13$ .

### 3.3 The plane velocity $U_m$

Figure 6 represents the vector lines of the velocity  $U_m$  in the symmetrical plane A-A at 10° before TDC for the axisymmetrical case as well as for the eccentricity values of 10.5, 20 and 30 mm. The case of 10.5mm in this figure is taken from [12] for comparison. The point in figure 6 indicates the position of the calculated velocity and the line gives the magnitude and direction of it with respect to the piston. Figure 6 shows that the air jet is bent at the corners tip of the bowl and by the symmetrical bowl two vortices are formed in the bowl. An anti-clockwise vortex is formed at the right half of the bowl and another clockwise one is formed at the left side of the bowl. By the increase of the eccentricity the air jet squish flow velocity at the right side diverts at the upper part of the bowl

thereby the anti-clockwise vortex becomes greater and the clockwise vortex becomes smaller.

Figure 7 shows the contour lines of the velocity  $U_{\theta}$  in the symmetrical section A-A at  $10^{\circ}\text{CA}$  before TDC for the eccentricities of  $e=0, 10.5, 15,$  and  $20$  mm. The case of  $e=10.5$  mm in this figure is taken from [12] for comparison. Along the bowl right side wall where the fuel is expected to be injected the velocity varies from 0 to 7.2 m/s by the symmetrical case where  $e=0$ , but with the increase of the eccentricity the variations of this velocity increase from 0 to 12 m/s by  $e=10.5$  mm and then takes nearly the same value from 0 to 12 by eccentricity values higher than 10.5 mm with a percentage increase of 137.5 with respect to the axisymmetric case. That means that the velocity gradient along the bowl right side wall increases with the increase of eccentricity to a certain limit.

Figure 7 shows also that the maximum velocity in the symmetrical plane A-A increases with the increase of the eccentricity. It reaches 12, 13, 15, and 17 m/s for  $e=0, 10.5, 15,$  and  $20$  mm respectively. The location of the maximum velocity changes also with the increase of the eccentricity. It locates by the axisymmetrical case at the core of the flow in two positions in the two sides of the piston cavity, but as the eccentricity increases to the left side of the cavity the maximum velocity occurs only in the right half of the cavity and its position deviates towards the piston top level.

Figures 6 and 7 show that with the increase of the eccentricity the center of the anti-clockwise swirl vortex moves vertically towards the cylinder top and horizontally towards the axis of the bowl while the center of the clockwise swirl vortex moves vertically down towards the bottom of the bowl and horizontally towards the left side wall.

#### 3.4 The plane velocity $U_{\theta}$

Figure 8 and 9 represent the vector and contour lines of the velocity  $U_{\theta}$  at  $10^{\circ}\text{CA}$  before TDC for the plane which is nearly located at one third of the bowl height  $k=9$ . The points in figure 8 indicate the location of the calculated velocities and the lines give the magnitudes and directions of it. Both figures show that the swirl center which coincides with the bowl center by the axisymmetrical case deviates by the increase of the eccentricity from its position away but nearly in the same direction. This deviation increases with the increase of the eccentricity. The increase of eccentricity creates also another two regions of maximum, and minimum velocities. The maximum velocity increases by the increase of the eccentricity from 12.6 m/s by the eccentricity of 10.5 mm to 14.4 and nearly 16.2 m/s by the eccentricity of 15 and 20 mm respectively, while the minimum velocity decreases from 9 m/s to 7.2 and 5.4 m/s by the eccentricities 10.5, 20 and 30 mm respectively.

#### 4. CONCLUSION

In the present study further computations are made to give better understanding of the in-cylinder air flow and to get the influence of the eccentricity of the bowl axis on the in-cylinder flow in a deep-bowl direct injection chamber during the compression stroke. The main points drawn from the present study may be summarized as follows:

1. The eccentricity causes change of the squish flow velocity along the tip of the piston cavity. It takes its maximum value at one side of the piston cavity till its minimum value at the other side.
2. The maximum value of the squish flow velocity increases with the increase of the eccentricity.
3. The change of the tangential velocity due to the increase of the eccentricity becomes always smaller with the proceeding of the flow towards the bottom of the cavity.
4. By the increase of the eccentricity one vortex in the bowl becomes greater and the other one becomes smaller.
5. The velocity gradient at the bowl wall where the fuel is expected to be injected increases with the increase of the eccentricity to a certain limit.

#### 5. NOMENCLATURE

$A_n$	area of the vertical plane between the squish volume and the combustion volume
$A_p$	the piston area
$e$	eccentricity of the bowl axis
$h$	piston position from the cylinder top
$h_c$	total cylinder length ( $h$ at BDC)
$K$	number represents the planes of the cylinder
$r$	radial coordinate
$r_b$	bowl radius
$R$	piston radius
$R_c$	piston radius measured from the bowl axis
$S_p$	mean piston speed
$U$	squish flow velocity
$U_m$	mean squish flow velocity over the area $A_n$
$U_c$	the squish flow velocity along the tip of the piston cavity which is equal to $U_m$ for the case of axisymmetrical cavity
$U_{r\theta}$	the velocity in the $r-\theta$ plane
$U_{rz}$	the velocity in the $r-z$ plane
$V$	tangential flow velocity
$V_c$	combustion volume which consists of the cavity volume plus the volume of the space over the cavity
$V_e$	the volume of the space between the piston ring and the cylinder head
	the ratio of the cavity volume to the clearance volume (cylinder volume at the TDC)
$\theta$	tangential coordinate
$\omega_0$	swirl ratio, the ratio of swirl angular velocity to that of the engine speed

## 6. REFERENCES

1. Ikegami, M., Horibe, K. and Komatsu, G., "Numerical simulation of flows in an engine cylinder (2nd. Report, flow in a deep-bowl combustion chamber)." Bulletin of JSME, Vol. 29, No. 250, April 1986.
2. Gosman, A.D. and John, R.J.R., SAE paper no. 800091 1986.
3. Ramos, J.I., Humphery, J.A.C. and Sirignano, N.A., SAE paper No. 790356 (1979)
4. Griffin, M.D., Anderson, J.D., Diwaker, R., "Navier-Stokes solutions of flow field in an I.C.E." AIAA Journal, Vol. 14 Dec. 1976 pp 1665-1666.
5. Seppen, J.J., "A study of flow field phenomena in I.C.E." Dissertation, H Delft oct. 1982.
6. Borgnakke, C., Davis, G.C., and Tabaczynski, R.J., "Predictions of in-cylinder swirl velocity and turbulence intensity of an open chamber cup in piston engine." SAE paper 810224, SAE Transaction Vol. 90, 1981.
7. El Kady, M.S., Mascheck, H.J., and Hoche A. "Numerical simulation of the flow in a symmetrical deep bowl combustion chamber of a diesel engine cylinder during the compression stroke" MEJ, Vol. 12 No. 2, Dec. 1987, pp M20-M30.
8. Markatos, N.C., and Shah, P., "Turbulence Modelling in internal combustion engines". Proceedings of the fourth international conference "Numerical methods in laminar and turbulent flow" held at Swansea 9th-12th July, 1985.
9. Schapertons, H., and Thiele, F., "three-dimensional computations for flow fields in DI piston bowls" SAE paper 860463, SAE 1986.
10. El Kady, M.S., Mascheck, H.J., and Hoche A. "Numerical simulation of flows in an engine cylinder with an eccentric deep bowl combustion chamber during compression. 1st Report, Formulation and algorithm)" to be published in the Egyptian Journal of Combustion 1988.
11. Fitzgeorge, D., and Allison, J.L., "Air swirl in a road-vehicle diesel engine." Proc. Instn. Mech. Engrs. Vol. 25, 1962, pp. 151-168.
12. El Kady, M.S., Mascheck, H.J., and Hoche A. "Numerical simulation of flows in an engine cylinder with an eccentric deep bowl combustion chamber during compression. (2nd Report, Numerical example)" to be published in the Egyptian Journal of Combustion 1988.

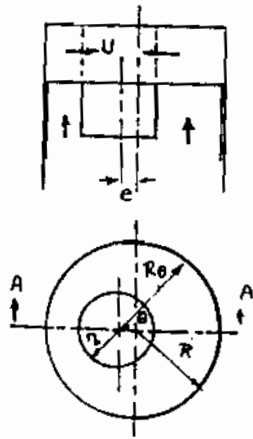


Fig. 1: Schematic of the bowl-in-piston chamber

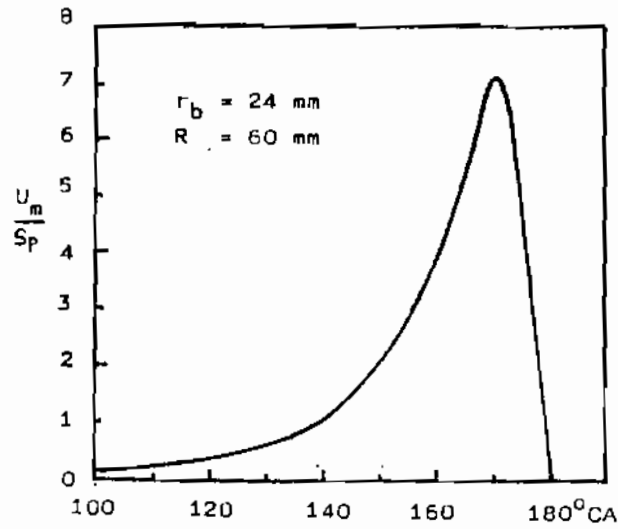


Fig. 2: Theoretical mean squish velocity divided by the mean piston speed for axisymmetric bowl-in-piston chamber for equation (3) during compression

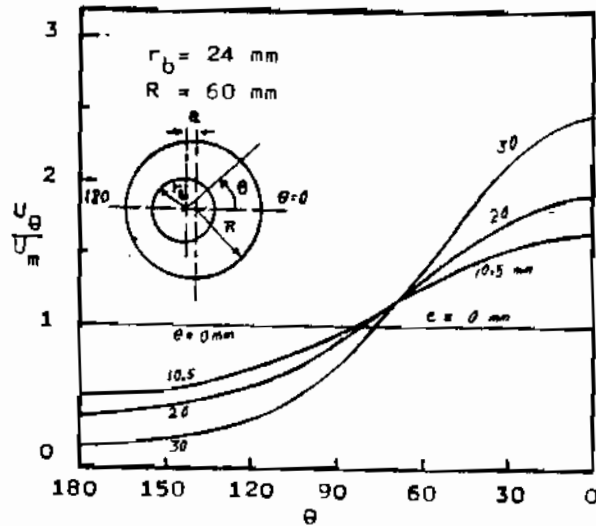


Fig. 3: Theoretical squish flow velocity divided by the mean squish velocity for the different angles  $\theta$  for different eccentricities during compression



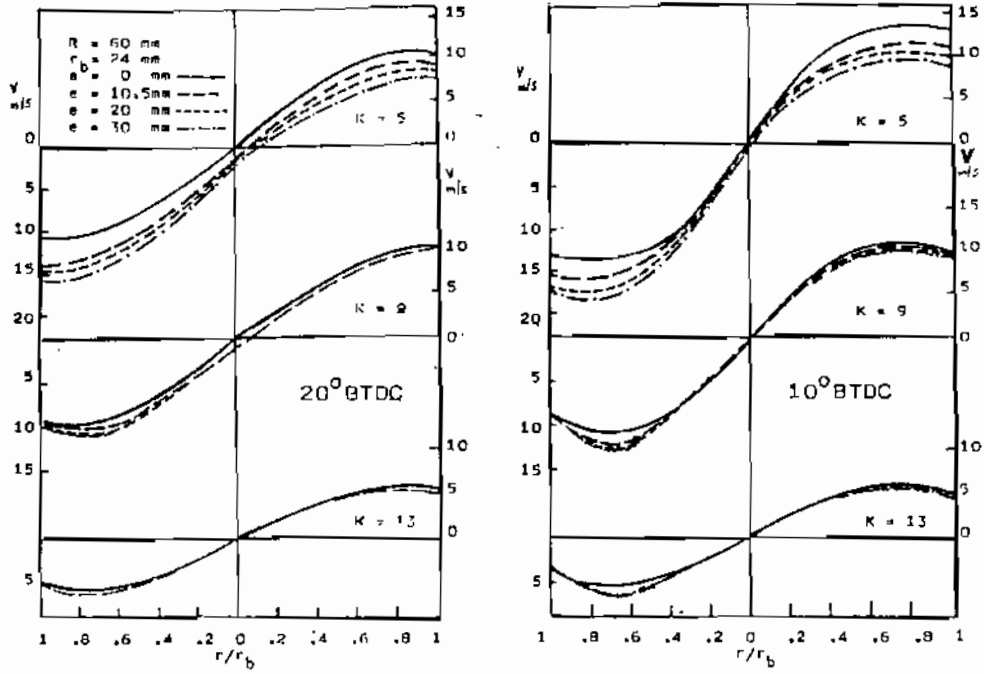


Fig. 5: The tangential flow velocity in the bowl-in-piston chamber at the symmetrical plane A-A for different sections and different eccentricities

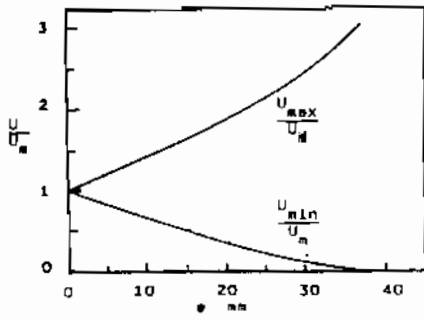
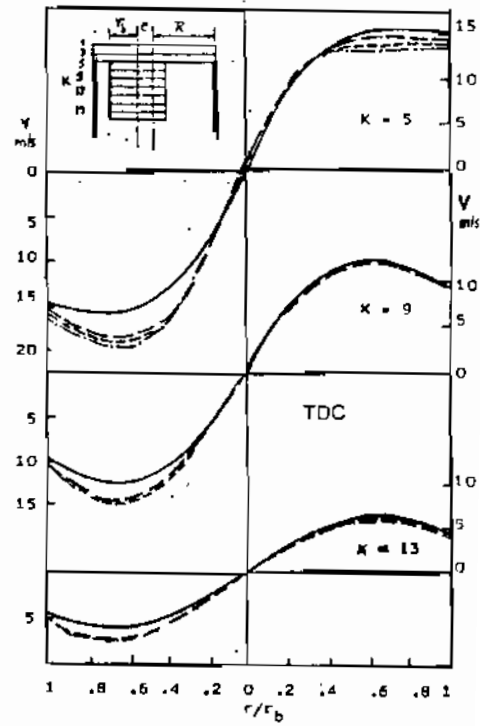


Fig. 4: The maximum and minimum values of the squish flow velocity for the different eccentricities.



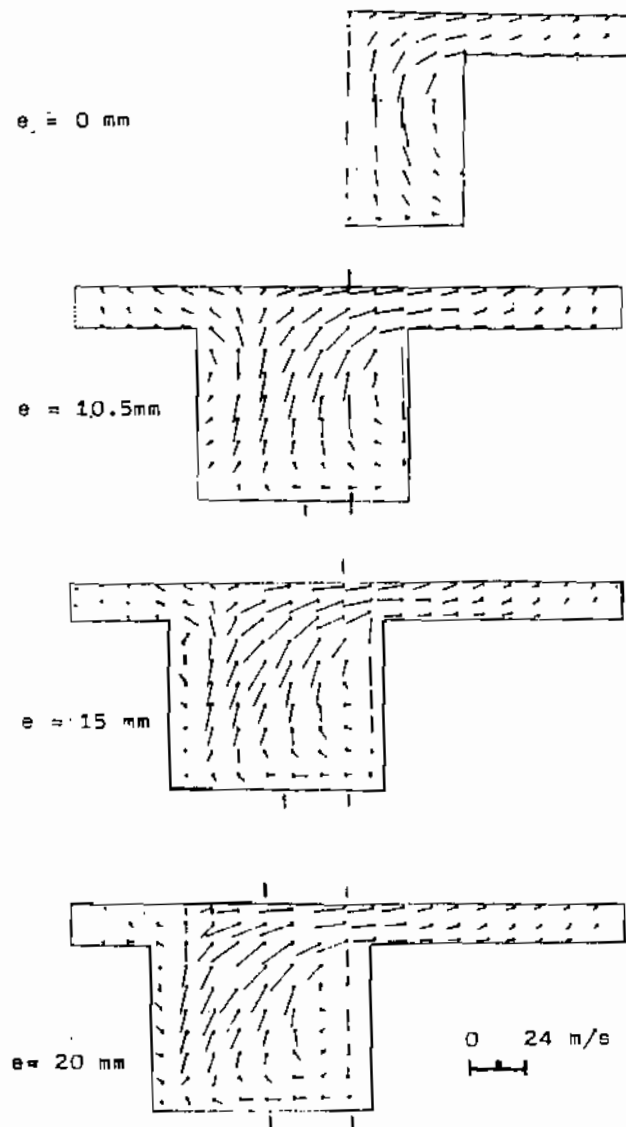


Figure 6 : The vector lines of the velocity  $U_{x,y}$  in the symmetrical plane A-A at  $10^\circ\text{CA BTDC}$

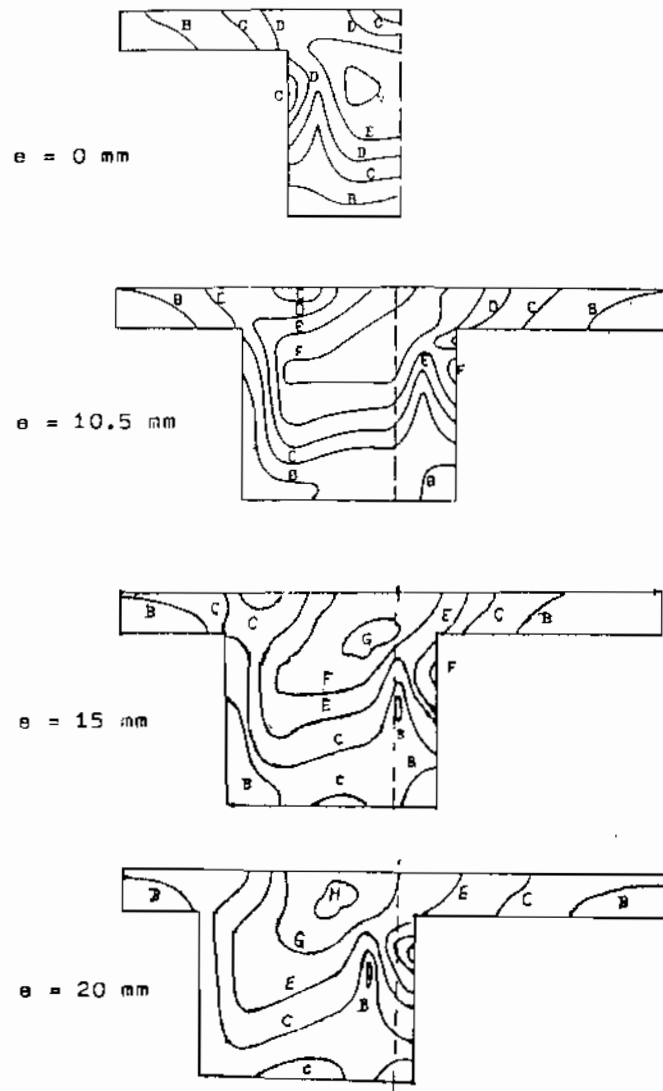


Figure 7: The contour lines of the velocity  $U_{rz}$  in the symmetrical section A-A at  $10^\circ$  CA BTDC  
 A = 0 , B= 2.4 , C= 4.8 , D=7.2 , E= 9.6  
 F = 12 , G= 14.4 , H= 16.8 m/s

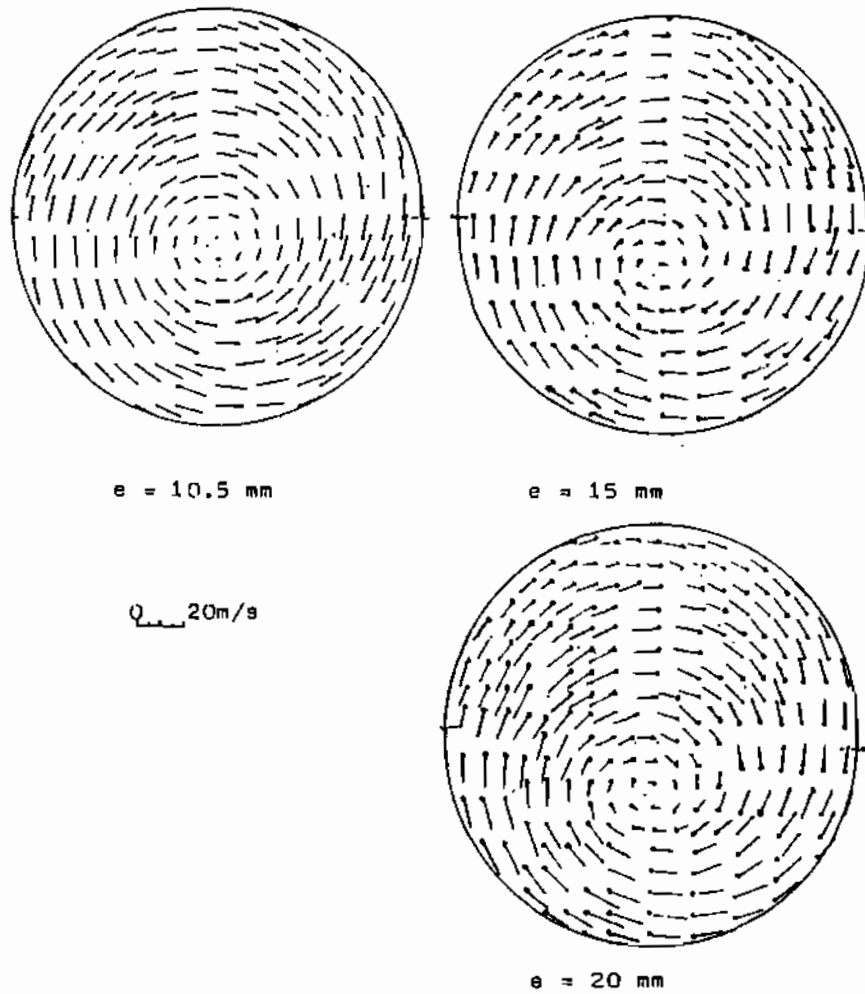


Figure 8: The vector lines of the velocity  $U_{re}$  at  $10^\circ$ CA BTDC and  $k=9$

